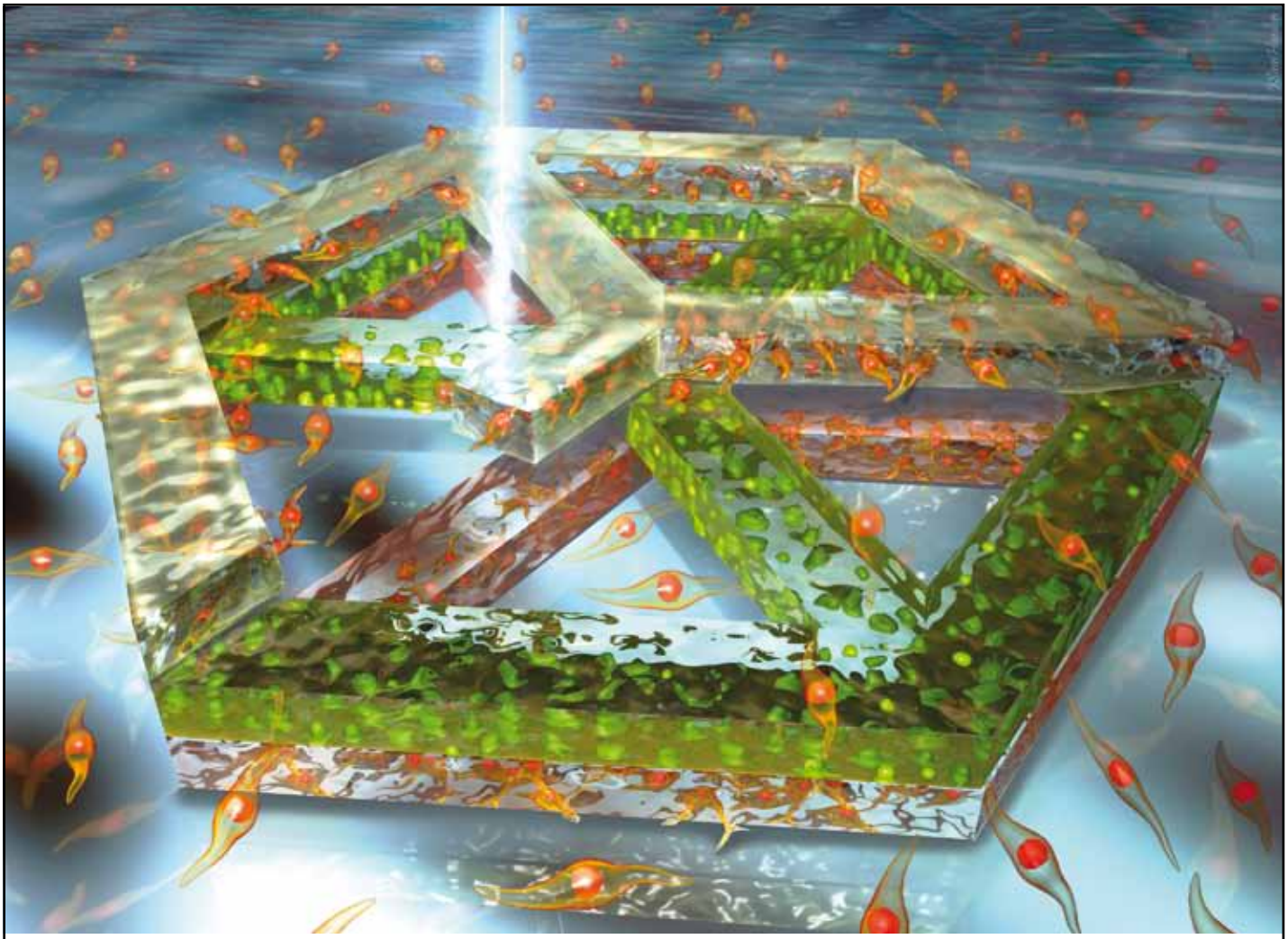

Featuring work from the group of Professor R. Bashir in the Department of Bioengineering, Department of Electrical and Computer Engineering, and the Micro and Nanotechnology Laboratory at the University of Illinois, Urbana-Champaign, Urbana, IL USA.

Title: Three-dimensional photopatterning of hydrogels using stereolithography for long-term cell encapsulation

Adapting stereolithographic technology for long-term encapsulation of living cells in complex 3D hydrogels. The spatial distribution of cells and bioactive molecules can be controlled by repetitive deposition and processing of individual layers using computer-controlled devices. Image courtesy of Janet Sinn-Hanlon at the Beckman Institute, University of Illinois at Urbana-Champaign.

As featured in:

See Bashir *et al.*, *Lab Chip*, 2010, **10**, 2062–2070

RSC Publishing

www.rsc.org/loc

Registered Charity Number 207890

Three-dimensional photopatterning of hydrogels using stereolithography for long-term cell encapsulation†

Vincent Chan,[ad] Pinar Zorlutuna,[ad] Jae Hyun Jeong,[b] Hyunjoon Kong[b] and Rashid Bashir*[acd]

Received 16th March 2010, Accepted 11th June 2010
DOI: 10.1039/c004285d

Cell-encapsulated hydrogels with complex three-dimensional (3D) structures were fabricated from photopolymerizable poly(ethylene glycol) diacrylate (PEGDA) using modified 'top-down' and 'bottoms-up' versions of a commercially available stereolithography apparatus (SLA). Swelling and mechanical properties were measured for PEGDA hydrogels with molecular weights (M_w) ranging from 700 to 10 000 Daltons (Da). Long-term viability of encapsulated NIH/3T3 cells was quantitatively evaluated using an MTS assay and shown to improve over 14 days by increasing the M_w of the hydrogels. Addition of adhesive RGDS peptide sequences resulted in increased cell viability, proliferation, and spreading compared to pristine PEG hydrogels of the same M_w. Spatial 3D layer-by-layer cell patterning was successfully demonstrated, and the feasibility of depositing multiple cell types and material compositions into distinct layers was established.

Introduction

The need for *in vitro* 3D model systems that can substitute for specific tissues is becoming increasingly prevalent in applications ranging from fundamental scientific studies, cancer metastases, stem cell biology, drug discovery, and the replacement of organs.[1] Native tissues are composed of heterogeneous mixtures of cell types and extracellular matrix (ECM) molecules that are arranged in complex 3D hierarchies and supported by an intricate network of blood vessels. Mimicking the spatial organization of these cells and ECM molecules is one of the major challenges toward developing tissue equivalents.

Hydrogels have been of particular interest as biomaterial scaffolds in these systems because of their close resemblance to native tissues. They are crosslinked polymer networks that are highly hydrated and possess tissue-like elasticity.[2,3] In particular, poly(ethylene glycol) (PEG) is a synthetic hydrogel that has been widely used because of its hydrophilicity, biocompatibility, and ability to be chemically tailored.[4] Cell adhesion domains,[5,6] growth factors,[7] and hydrolytic[8] and proteolytic[9,10] sequences have also been incorporated into PEG hydrogels to guide cellular processes such as differentiation, proliferation, and migration. By modifying the ends with either acrylates or methacrylates, PEG hydrogels can be photocrosslinked in the presence of appropriate initiating agents.[11,12] This type of curing offers spatial control over polymerization that, while increasingly popular,[13–15] has not been fully exploited.

Computer-aided design (CAD)-based rapid prototyping technologies have recently been applied as enabling tools that provide excellent spatial control over scaffold architecture.[16,17] Rapid prototyping is the process of creating complex 3D structures by repetitive deposition and processing of individual layers using computer-controlled devices. Usually, a blueprint is developed first and translated into a 3D design in a format that can be used by the rapid prototyping system. The design is sliced into a collection of 2D cross-sectional layers that is then processed into a real 3D structure using layer-by-layer deposition. By controlling the micro- and macro-architecture of these scaffolds, rapid prototyping technologies can potentially be used to create artificial vasculature to facilitate the flow of oxygen and nutrients into the construct, thereby increasing the potential size of the tissue.[18,19] Additionally, angiogenic factors can be added to the vasculature to induce the formation of new blood vessels.[20] Because of their excellent spatial control, it is possible to create 3D structures with multi-cellular components that are required for complex tissue function.[21–23] Furthermore, rapid prototyping technologies provide a means for large-scale production of reproducible tissue constructs that can be used in a variety of applications.

A common issue in the vast majority of rapid prototyping technologies is the acellular environment in which the scaffolds are fabricated in. Because cells cannot survive these processing conditions, they are normally seeded on top of the scaffolds and induced to migrate and populate into the inner regions. In this approach, however, it is often difficult to obtain scaffolds that are evenly seeded with cells.[24] An approach where it might be possible to entrap cells in the scaffolds during the fabrication process would be very advantageous because of their homogeneous distribution. One of the technologies that may be mild enough to encapsulate living cells during the fabrication process is stereolithography.

The conventional stereolithography apparatus (SLA) uses ultraviolet (UV) light to selectively solidify photosensitive

[a]*Department of Bioengineering, University of Illinois at Urbana-Champaign, Urbana, Illinois, 61801, USA*
[b]*Department of Chemical and Biomolecular Engineering, University of Illinois at Urbana-Champaign, Urbana, Illinois, 61801, USA*
[c]*Department of Electrical and Computer Engineering, University of Illinois at Urbana-Champaign, Urbana, Illinois, 61801, USA*
[d]*2000 Micro and Nanotechnology Laboratory, University of Illinois at Urbana-Champaign, MC-249, 208 North Wright Street, Urbana, Illinois, 61801, USA. E-mail: rbashir@illinois.edu; Fax: +1 (217) 244-6375; Tel: +1 (217) 333-3097*

† Electronic supplementary information (ESI) available: Fig. S1–S5 and other experimental details. See DOI: 10.1039/c004285d

polymers. There are two main approaches in the SLA: (1) masked-based writing and (2) direct or laser writing. Photopolymerizable PEG diacrylate (PEGDA) hydrogels have been used to encapsulate hepatocytes for up to 7 days in masked-based writing methods, which employ a flood lamp to shine UV light through the openings of a mask.[15] This method requires lots of masks to create a complex structure, and it is difficult to control the amount of energy that the cells are being exposed to in each layer. Direct-writing approaches, which employ a UV laser to selectively cure the liquid polymer in a predetermined manner, have also been explored with hydrogels recently.[25–28] However, long-term viability of cells encapsulated within these hydrogels has not yet been demonstrated.

In this study, a commercially available SLA was modified to accommodate for two fabrication methods: (1) the 'top-down' approach, which employs a process similar to the conventional SLA, and (2) the 'bottoms-up' approach, which allows for multiple cell types and material compositions to be arranged in their own layers within a structure. Laser polymerization characteristics of PEGDA hydrogels were examined and optimized for their utilization in the SLA. The swelling and mechanical properties of these hydrogels were measured as a function of M_w. Long-term viability, proliferation, and spreading of encapsulated NIH/3T3 cells over 14 days were evaluated in single-layer and multi-layer 3D structures prepared from PEGDA hydrogels with a range of M_w and RGDS peptide sequences. Furthermore, controlled spatial distribution of cells and bioactive molecules in distinct layers was achieved by exploiting the capabilities of the 'bottoms-up' SLA approach.

Materials and methods

Apparatus

A stereolithography apparatus (SLA, Model 250/50, 3D Systems, Rock Hill, SC, USA) was used for all experiments. Modifications were made to accommodate for two types of fabrication processes as shown in Fig. 1. In the 'top-down' approach, the standard vat and platform were removed to allow for low volume materials, including those containing living cells. A smaller custom-made mini-platform was fabricated and screwed into an aluminium shaft that was clamped to the elevator of the SLA. In the 'bottoms-up' approach, the vat was removed and replaced with a 35 mm diameter culture dish. The dish was placed at the center of the platform with an 18 mm^2 cover glass bonded to the bottom to allow the cured hydrogel to temporarily attach to it during processing. This method was used for layering multiple cell types and material compositions in distinct regions of the structure.

Cell culture

NIH/3T3 cells (ATCC, Manassas, VA, USA) were cultured in Dulbecco's modified Eagle's medium (DMEM, Sigma Aldrich, St Louis, MO, USA) containing 4.5 g L^{-1} glucose and supplemented with 10% fetal bovine serum (FBS, Sigma Aldrich, St Louis, MO, USA), 100 U mL^{-1} penicillin, and 100 μg mL^{-1} streptomycin (Gibco, Carlsbad, CA, USA). Cells were incubated in 175 cm^2 flasks (Fisher Scientific, Springfield, NJ, USA) at 37 °C and 5% CO_2. Cells grown to pre-confluency were passaged

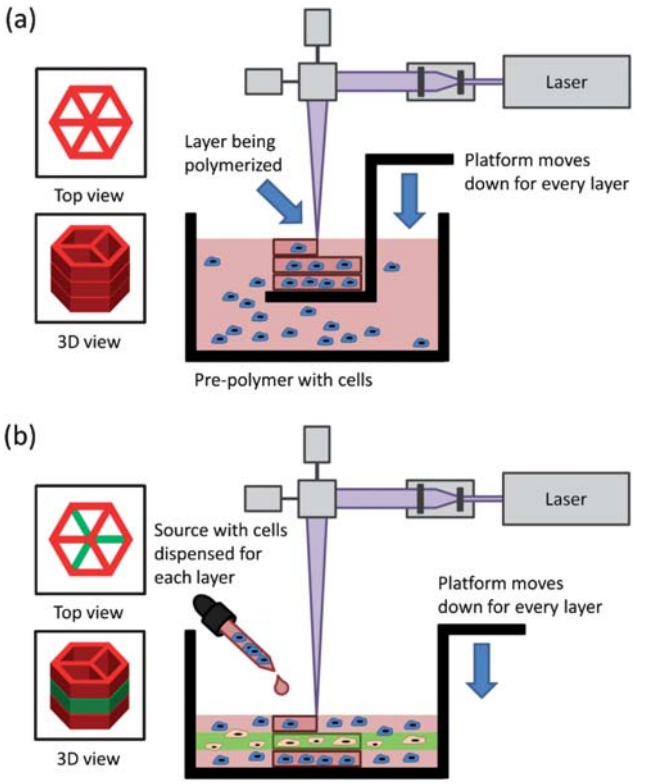

Fig. 1 A schematic representation of the SLA modifications. (a) In the top-down approach, the layout consists of a platform immersed just below the surface of a large tank of pre-polymer solution. After the layer is photopolymerized, the platform is lowered a specified distance to recoat the part with a new layer. (b) In the bottoms-up approach, the pre-polymer solution is pipetted into the container one layer at a time from the bottom to the top. This setup was modified especially for cell encapsulation applications, which required: (1) reduction in total volume of photopolymer in use and (2) removal of photopolymer from static conditions that cause cells to settle.

no more than 10 times using 0.25% trypsin and 0.04% EDTA in HBSS (Gibco, Carlsbad, CA, USA). Prior to encapsulation in hydrogels, cells were added to the pre-polymer solution and mixed gently. For multi-cell type layering, cells were split into two separate suspensions and labeled with either CellTracker® CMFDA or CMTMR fluorescent dyes (Molecular Probes, Eugene, OR, USA).

Pre-polymer preparation

Poly(ethylene glycol) diacrylates (PEGDAs) of M_w 700 (Sigma Aldrich, St Louis, MO, USA), 3400, 5000, and 10 000 Da (Laysan Bio, Arab, AL, USA) were dissolved in DMEM without phenol red (Gibco, Carlsbad, CA, USA) to form a 40% (w/v), or 2X, pre-polymer solution. The photoinitiator, 1-[4-(2-hydroxy-ethoxy)-phenyl]-2-hydroxy-2-methyl-1-propane-1-one (Irgacure 2959, Ciba, Tarrytown, NY, USA), was dissolved in dimethyl sulfoxide (DMSO, Fisher Scientific, Springfield, NJ, USA) at 50% (w/v) stock solution and added to the 2X pre-polymer solution to form 1.0% (w/v) of photoinitiator. Medium with or without cells and 20% fetal bovine serum (FBS, Sigma Aldrich, St Louis, MO, USA) were added to the pre-polymer solution in

a 1 : 1 volumetric ratio prior to each SLA run. The final pre-polymer solution consisted of 20% (w/v) PEGDA, 0.5% (w/v) photoinitiator, and 10% FBS in DMEM without phenol red. For studies with bioactive groups, RGDS peptide sequences (Arg-Gly-Asp-Ser, Sigma Aldrich, St Louis, MO, USA) were conjugated to acrylate-PEG-NHS (M_w 3500, JenKem Technology, Allen, TX, USA).[15] Acryloyl-PEG-RGDS was added to the pre-polymer solution to make a final concentration of 5 mM RGDS.

Sequential layer-by-layer hydrogel photopatterning

CAD models were generated using AutoCAD 2009 (Autodesk, San Rafael, CA, USA) and exported to stereolithography (STL) format. The SLA software, 3D Lightyear v1.4 (3D Systems, Rock Hill, SC, USA), was used to slice the 3D models into a series of 2D layers from a user-specified thickness. The penetration depth (D_p) and critical exposure energy (E_c) parameters, which are constants specific to a desired pre-polymer solution, were acquired from energy dose characterizations (see ESI†) and entered into the SLA software. For the 'top-down' fabrication process, the platform was immersed just below the surface of the pre-polymer solution with or without cells. For the 'bottoms-up' fabrication process, the pre-polymer solution with or without cells was pipetted into the culture dish at the correctly characterized volume (Fig. S2†). The laser was used to selectively crosslink the pre-polymer solution at a precisely calculated energy dose. The elevator controlled by the SLA was lowered by a specified distance, and the part was recoated. The process was repeated until completion of the complex 3D structure. The structure was rinsed several times in the appropriate medium to remove uncrosslinked polymer.

Hydrogel characterization

Gel disks fabricated in the SLA were subjected to compression using a mechanical testing system (Insight, MTS Systems, Eden Prairie, MN, USA). The elastic modulus (E) of the gel was measured by compressing at a constant deformation rate of 1.0 mm s^{-1} at 25 °C. From the strain limit to the first 10%, the elastic modulus was calculated using the slope of the stress (σ) *vs.* strain (λ) curve. Assuming that the gels follow an affined network model, the shear modulus (S) was calculated from the slope of the σ *vs.* $-(\lambda - \lambda - 2)$ curve, where λ is the ratio of the deformed length to the undeformed length of the hydrogel.[10,29]

The swelling ratios of the gels at equilibrium were determined by measuring the weight of the swollen gels after 24 hours in pH 7.4 buffer solutions at 37 °C and the weight of the dried gels. The degree of swelling (Q), defined as the reciprocal of the volume fraction of a polymer in a hydrogel (ν_2), was calculated from the following equation,

$$Q = \nu_2^{-1} = \rho_P\left(\frac{Q_m}{\rho_S} + \frac{1}{\rho_P}\right) \quad (1)$$

where ρ_S was the density of water, ρ_P was the density of polymer, and Q_m was the swelling ratio, the mass ratio of swelled gel to dried gel.

The average pore size (ξ) was calculated from the polymer volume fraction ($\nu_{2,s}$) and the unperturbed mean-square end-to-end distance of the monomer unit (r_o^{-2}) using eqn (2) and (3):

$$\xi = \left(\nu_{2,s}^{-1/3}\right)\left(r_o^{-2}\right)^{1/2} \quad (2)$$

$$\left(r_o^{-2}\right) = l\left(2\frac{\overline{M_c}}{M_r}\right)^{1/2} C^{1/2} = l(2n)^{1/2}C^{1/2} \quad (3)$$

where l is the average value of the bond length between C–C and C–O bonds in the repeatable unit of PEG [–O–CH_2–CH_2–], which is taken as 1.46 Å; M_c is the average molecular mass between crosslinks in the network; M_r is the molecular mass of the PEG repeating unit (44 g mol^{-1}); C is the characteristic ratio for PEG, which is taken here as 4.

Cell viability

Cell viability was quantitatively measured using MTS (3-(4,5-dimethylthiazol-2-yl)-5-(3-carboxymethoxyphenyl)-2-(4-sulfophenyl)-2*H*-tetrazolium, Promega, Madison, WI, USA), a tetrazolium compound which, in the presence of phenazine methosulfate (PMS, Sigma Aldrich, St Louis, MO, USA), is reduced by living cells to yield a water-soluble formazan product. MTS (333 μg mL^{-1}) and PMS (25 μM) were added to the cell-laden hydrogels in DMEM without phenol red in an incubator at 37 °C and 5% CO_2. After incubating for 4 hours, 20% SDS (Fisher Scientific, Springfield, NJ, USA) in sterilized H_2O^{dd} was added to stop the reaction. The hydrogels were incubated at 37 °C for 15 hours to allow diffusion of formazan into the medium. The absorbance was measured at 490 nm using a Synergy HT microplate reader (BioTek, Winooski, VT, USA). Viability was qualitatively evaluated in stereomicroscopy using an MTT assay (3-(4,5-dimethylthiazol-2-yl)-2,5-diphenyltetrazolium bromide, Sigma Aldrich, St Louis, MO, USA) by incubating the cell-laden hydrogels in a 10% solution of DMEM without phenol red at 37 °C and 5% CO_2 for 4 hours. Fluorescence microscopy using calcein AM and ethidium homodimer stains was also used for qualitative evaluation (Molecular Probes, Eugene, OR, USA).

Cell spreading

In order to visualize spreading, cell-laden hydrogels were examined every day by bright-field microscopy. After 14 days, cells were fixed using 4% formaldehyde solution (Fisher Scientific, Springfield, NJ, USA) overnight at room temperature. After washing several times in PBS, the gels were incubated in Triton X-100 (Sigma Aldrich, St Louis, MO, USA) for 20 min and stained with rhodamine phalloidin (Molecular Probes, Eugene, OR, USA) and 4′,6-diamindino-2-phenylindole (DAPI, Sigma Aldrich, St Louis, MO, USA) for 30 minutes at 37 °C. The cells were imaged using an inverted fluorescent microscope (IX81, Olympus, Center Valley, PA, USA).

Statistical analysis

Error bars represent standard deviation, with $n = 3$ for all experiments. Statistical significance was determined using one-way ANOVA followed by Tukey's Multiple Comparison Test ($P < 0.05$).

Results

Swelling and mechanical properties of hydrogels

The degree of swelling and the mechanical properties of laser-polymerized PEGDA hydrogels were investigated as a function of M_w. At the time of the study, the laser power of the SLA was about 15 mW and the average energy dose used to photo-polymerize the gel disks was 1600 mJ cm^{-2}. The swelling ratios (Q) and elastic moduli (E) for 20% (w/v) PEGDA hydrogels with M_w 700, 3400, 5000, and 10Å000 Da were measured and calculated from these gel disks (Fig. 2). As expected, the Q increased and the E decreased with increasing PEG M_w. The swelling ratios were also used to calculate the average pore size of the gel disks as a function of M_w (Table 1). The elastic moduli obtained ranged from 4.73 ± 0.46 kPa for M_w 10 000 Da to 503 ± 57 kPa for M_w 700 Da, which covers quite an array of native tissues having similar moduli.[30] Stereomicroscopic images of PEG hydrogels after 24 hour incubation in cell culture medium showed an increase in swelling capacity with increasing M_w (Fig. S3†).

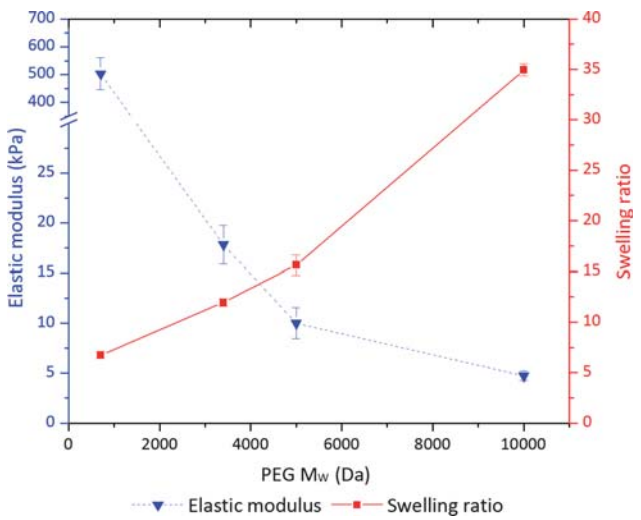

Fig. 2 Mechanical properties and swelling of laser-polymerized PEGDA hydrogels. The elastic moduli (E, left axis) and swelling ratios (Q, right axis) were measured and calculated for 20% PEGDA hydrogels as a function of M_w (700, 3400, 5000, and 10 000 Da). All experiments used 0.5% photoinitiator concentration.

Table 1 Calculated average pore size of laser-polymerized PEGDA hydrogels as a function of M_w. The average pore size of 20% PEGDA hydrogels with M_w 700, 3400, 5000, and 10 000 Da was calculated from values obtained by measuring the swelling ratios of gel disks with a diameter of 5 mm. The pore size increased as a function of increasing M_w

PEG M_w/Da	Pore size/nm
700	3.105
3400	8.280
5000	10.973
10 000	20.340

Cell encapsulation

Cell encapsulation was initially accomplished by using the 'top-down' fabrication process, which held all the pre-polymer solution in a stationary container. A 2 mm thick complex 3D structure, which was composed of 20 layers (100 μm per layer), was fabricated using this approach (Fig. 3(a)). The distribution of cells embedded within these structures was examined using MTT stain and stereomicroscopy (Fig. 3(b)). The purple formazan crystals produced by the viable cells appeared to have an inhomogeneous distribution with more cells being embedded at the bottom of the structure than at the top of it. This was caused by cells that settled toward the bottom of the container due to gravity. To prevent this, the 'top-down' approach was altered, and the same complex 3D structure was fabricated using the 'bottoms-up' fabrication process. In this approach, the pre-polymer solution containing cells was pipetted into the container one layer at a time. The cells did not have time to settle to the bottom before the layer was cured. As a result, a uniform distribution of cells was achieved throughout the hydrogel, which was evident by the homogeneous distribution of purple formazan crystals (Fig. 3(c)). To quantitatively evaluate this, an intensity profile at different regions of the hydrogel was examined and confirmed to be uniform (Fig. 3(d)).

Cell viability

Two methods were used to evaluate long-term cell viability in the SLA: (1) encapsulation in single-layer 3D hydrogels (1 total layer, 1 mm thick per layer), and (2) encapsulation in multi-layer 3D hydrogels (10 total layers, 100 μm thick per layer).

In the first study, NIH/3T3 cells at a density of 2.0 × 10^6 cells mL^{-1} were encapsulated in 20% PEGDA hydrogels patterned in single-layer disks with dimensions of 1 mm thickness and 5 mm diameter. These disks were cultured over a period of 14 days. To achieve 1 mm thickness, the average energy dose of the laser during polymerization was 1000 mJ cm^{-2}. Cell viability was quantitatively evaluated using MTS assays. The optical density (OD) measurements obtained from these assays on 1, 4, 7, and 14 days were converted to relative cell viability (%) by normalizing to 0 day (Fig. 4).

Cells encapsulated in PEGDA hydrogels with M_w 700 Da survived the initial processing conditions of the SLA, but died within 24 hours of culturing. This was seen with and without 5 mM RGDS functionalization. By increasing the M_w to 3400 Da, cells survived both the processing and culturing conditions. Viability remained statistically constant through 4 days. Subsequently, there was a decrease in viability to 65.10 ± 9.81% after 7 days and to 47.46 ± 15.39% after 14 days. Adhesive RGDS peptide sequences at 5 mM concentration were chemically linked to PEGDA hydrogels with M_w 3400 Da to test for any improvement in cell viability and proliferation. This resulted in a 1.6-fold increase in cell numbers after 24 hours, which was maintained over 7 days. The effect of an even greater M_w on cell viability was also evaluated. Cells encapsulated in PEGDA hydrogels with M_w 5000 Da followed the same trend as that of M_w 3400 Da. Except for an unsustained rise in metabolic activity after 24 hours, the cell viability was relatively steady through 7 days, followed by a decrease in viability to 60.00 ± 0.2%

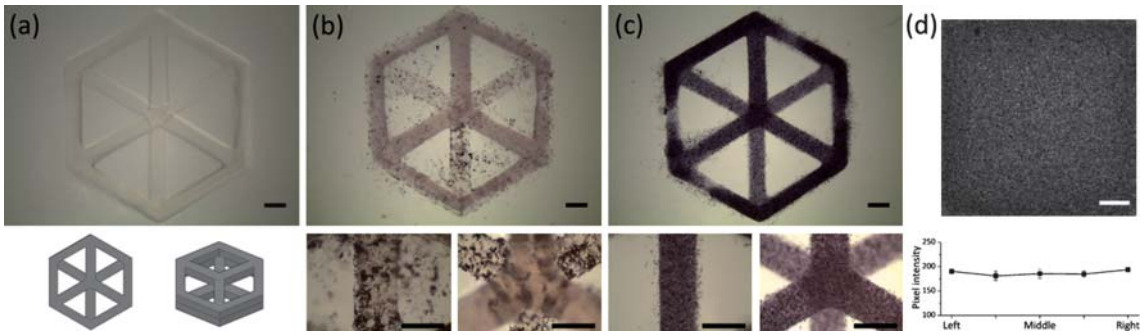

Fig. 3 Encapsulation of NIH/3T3 cells in laser-polymerized PEGDA hydrogels. (a) Fabrication of a 2 mm thick complex 3D structure composed of 20 layers (with CAD images). Two approaches were used to encapsulate 10×10^6 cells mL^{-1}: (b) top-down and (c) bottoms-up SLA modifications. Cells were immediately stained with MTT (over 4 hours) for visualization. In the top-down approach, cells settled to the bottom of the container and did not encapsulate well. In the bottoms-up approach, cells and pre-polymer were added before polymerization of each layer, which led to homogeneous and high cell densities. (d) Intensity measurements of an MTT stain quantitatively showed homogeneity throughout the structure immediately after encapsulation. Scale bars are 1 mm.

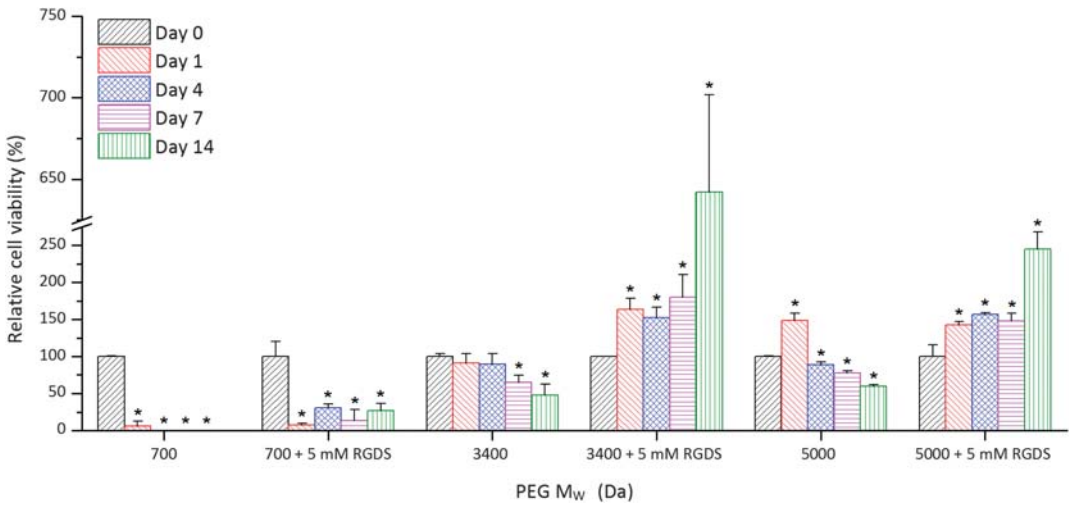

Fig. 4 NIH/3T3 cell viability over 14 days in PEGDA hydrogels with M_w 700, 3400, and 5000 ± RGDS groups. OD (490 nm) values quantified by MTS assays were normalized to 0 day. All values are mean ± standard deviation of $n = 3$. (*) denotes statistical difference compared to 0 day of same M_w.

viability after 14 days. This was an improvement over the 14 day viability of PEGDA hydrogels with M_w 3400 Da (47.46 ± 15.39%). When 5 mM RGDS was chemically linked to PEGDA hydrogels with M_w 5000 Da, there was a 1.4-fold increase in cell numbers after 24 hours, which was maintained over 7 days. A significant increase in viability was seen after 14 days for M_w 3400 and 5000 Da with RGDS peptide sequences due to high cell spreading, proliferation, and network formation on the exterior of the gels. Cell viability was also related to average pore size in Fig. S3†. The relative cell viability and proliferation generally increased with increasing average pore size.

Since cell viability in single-layer disks may not be truly representative of viability in complex 3D structures, the second study evaluated cells encapsulated in multi-layer 3D hydrogels over 14 days. RGDS peptide sequences at 5 mM concentration were chemically linked to PEGDA with M_w 5000 Da for this study. According to Fig. 5(a), the cell numbers were increased 1.7-fold after 24 hours, which was maintained through 7 days. By the end of 14 days, 46.44 ± 19.56% of the cells were viable. Distribution of cells in single-layer and multi-layer PEGDA M_w 5000 Da hydrogels can be seen from stereomicroscopic images of hydrogels subjected to MTT staining (Fig. 5(b) and (c)). Although there was a decrease in cell numbers after 14 days compared to 7 days, the distribution of the cells was homogeneous at both time points.

Qualitative LIVE/DEAD cell viability stain was performed during the same time points as the MTS assays. Representative images (Fig. S4†) showed an increase in the dead cells over later time points, which supported the results of the more quantitative MTS assays. Nevertheless, in all cases except PEGDA M_w 700 Da, the number of live cells was much more abundant than the number of dead ones.

Cell spreading

NIH/3T3 cells encapsulated within multi-layer PEGDA hydrogels with M_w 5000 Da were examined for cell spreading and attachment. Spreading, which involves the active processes of actin polymerization and myosin contraction,[31] is a sign of cell viability and function. Viable cells did not

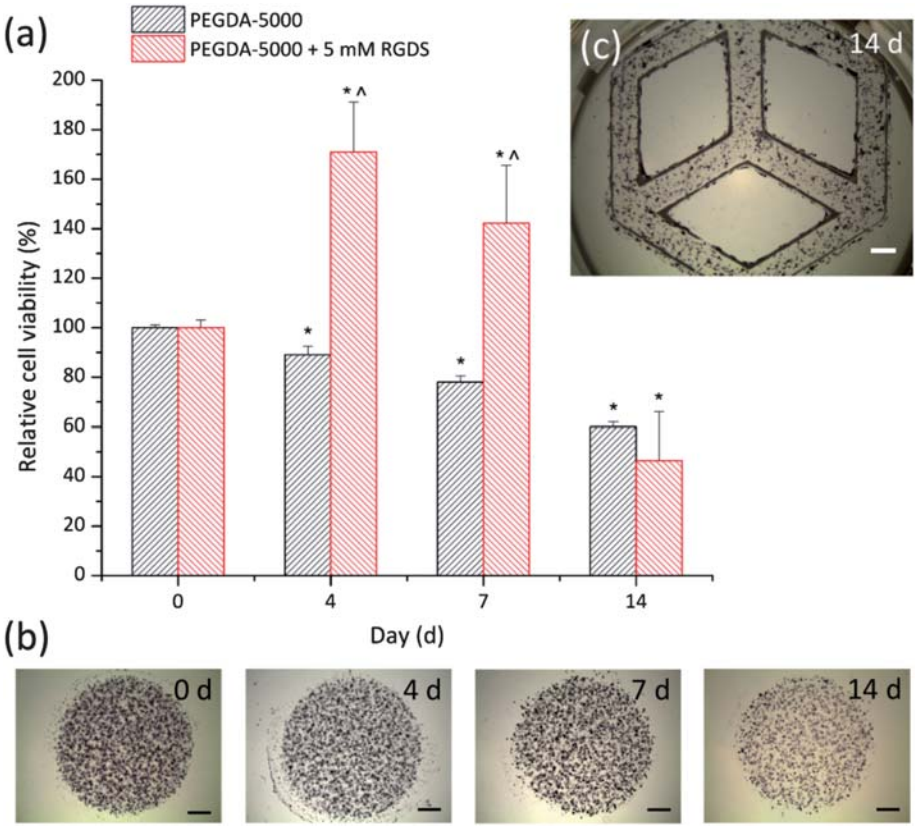

Fig. 5 NIH/3T3 cell viability over 14 days in PEGDA hydrogels with M_w 5000 using single-layer and multi-layer approaches. (a) OD (490 nm) values quantified with MTS assay were normalized to day 0. All values are mean ± standard deviation of $n = 3$. (*) denotes statistical difference compared to 0 day of same approach. (^) denotes statistical difference compared to different approach of same day. (b) MTT staining that shows living cells in a patterned multi-layer PEGDA hydrogel with M_w 5000 Da after 14 days. (c) MTT staining that shows living cells in single-layer PEGDA hydrogel disks with M_w 5000 Da after 0, 4, 7, and 14 days. There was a noticeable difference in intensity after 14 days. Scale bars are 1 mm.

spread in hydrogels without adhesive RGDS peptide sequences. Cells in multi-layer PEGDA hydrogels with RGDS-linked groups (5 mM) were examined in bright-field microscopy and fluorescence microscopy after rhodamine phalloidin (cytoskeleton) and DAPI (nuclei) staining (Fig. 6). Cell spreading was clearly seen within hours of incubation and continued through 14 days. Some of these cells formed 3D connections with other cells in different layers, suggesting network formation.

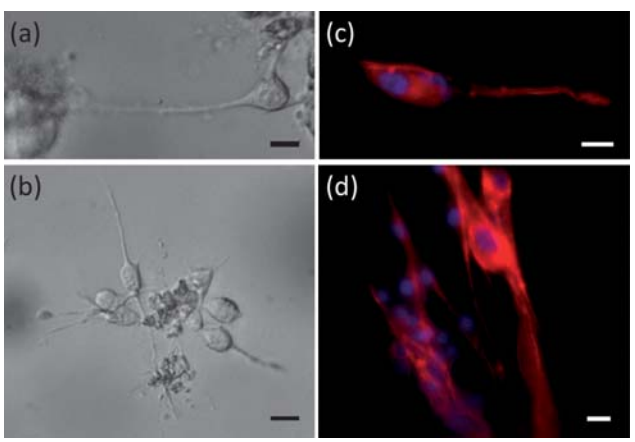

Fig. 6 NIH/3T3 cells spreading in laser-polymerized hydrogels containing bioactive RGDS groups. Single and clustered cells were clearly seen spreading in patterned multi-layer PEGDA hydrogels with M_w 5000 Da. These hydrogels were tailored with bioactive RGDS groups at a concentration of 5 mM. (a and b) Bright-field and (c and d) fluorescence microscopy images of the cells were taken after 14 days. For fluorescence microscopy, cells were fixed and stained with rhodamine phalloidin (cytoskeleton) and DAPI (nuclei). Scale bars are 20 μm.

Multi-cell type layering

The concept of incorporating multiple cell types within hydrogels in a spatially predetermined manner was demonstrated by using NIH/3T3 cells. These cells were separated into two suspensions: one labeled with CellTracker® CMFDA (green) fluorescent dye, and the other labeled with CellTracker® CMTMR (red) fluorescent dye. Fig. 7 illustrates top- and side-view fluorescent images of a complex 3D structure with overhangs containing two differently labeled cell suspensions. The thickness of each set of layers was uniform and showed minimal mixing. Quantitative results confirmed the distribution of these cells in uniformly distinct layers.

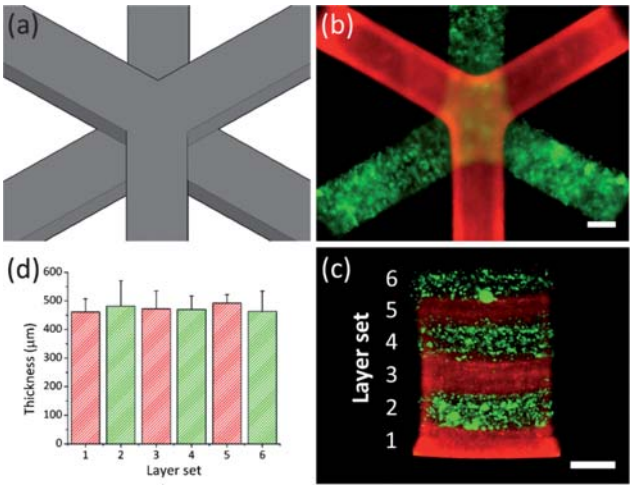

Fig. 7 Spatial 3D layer-by-layer cell patterning of viable cells at distinct layers. (a) CAD rendering of crosshatch pattern used for layer-by-layer spatial patterning. Each layer set was 1 mm thick (10 total layers, 100 μm each). (b) Fluorescence image of NIH/3T3 cells encapsulated on different layer sets stained with either CellTracker® CMFDA (green) dye or CMTMR (orange) dye. (c) Cross-sectional view of a block pattern consisting of alternating layer sets (5 total layers, 100 μm each). (d) Quantitative analysis of (c) showing layer sets comparable to the desired 500 μm thickness. All values are mean ± standard deviation of $n = 4$. Scale bars are 1 mm.

Discussion

Functional 3D tissues that are designed for individual patients using multi-cellular and multi-material compositions in an automated, high-throughput device will soon be the next generation in tissue engineering. The combination of process-optimized rapid prototyping technologies, such as stereolithography, with novel biomaterials may be one possible path toward this goal.

Cooke *et al.*[25] reported the use of stereolithography for tissue engineering applications by designing biodegradable scaffolds prepared from poly(propylene fumarate) (PPF) and diethyl fumarate (DEF). While this study demonstrated the capability of using photopolymerizable biomaterials in the SLA, cells were not seeded in or on any of these fabricated PPF/DEF structures. Subsequently, Dhariwala *et al.*[26] encapsulated Chinese hamster ovary (CHO) cells in poly(ethylene oxide) (PEO) and poly-(ethylene glycol) dimethacrylate (PEGDM) hydrogels. A fluorescence-based LIVE/DEAD assay was used to evaluate cells immediately after polymerization in the SLA, but the results lacked any substantive evidence supporting sustained viability or proliferation. Moreover, the cells were only encapsulated within single layer structures. This study also reported hydrogel samples with an average elastic modulus of 1.116 ± 0.21 kPa, which limits its applications to very soft tissue types.[30] In contrast, our own studies using 20% PEGDA hydrogels with M_w from 700 to 10 000 Da had elastic moduli that varied from 4.73 ± 0.46 kPa to 503 ± 57 kPa. These values are more suitable for a wider range of tissues.[30] Recently, Arcaute *et al.*[27] demonstrated complex 3D hydrogels in the SLA using low-swelling PEGDM hydrogels with M_w 1000 Da. Their viability studies were performed with human dermal fibroblasts (HDFs) encapsulated in gel disks for up to 24 hours. Similar to the previous study, these results were short-term and made with single-layers.

In this study, we demonstrated that NIH/3T3 cells encapsulated in both single-layer and multi-layer 3D hydrogels retained long-term viability, proliferation, and spreading over 14 days using the SLA. This is a significant step toward the development of rapid prototyping technologies for cell encapsulation applications. The SLA is advantageous because it allows for precise internal pore structures and defined macroscopic shapes, as well as the potential to control the spatial organization of multi-cellular and material compositions within the complex 3D structure. Studies in literature have investigated the behavior of various multi-cellular cultures within hydrogels. Although the cultures were shown to enhance desired cellular functions and behaviors, there was no real control over the spatial distribution of these cells.[32,33] Other studies have shown more controlled distribution, but with micropatterned 2D surfaces.[34,35] Since native tissues are composed of more than one cell type, the 'bottoms-up' SLA fabrication process described in our study can be used to study these multi-cellular cultures in defined 3D patterns.

The 'bottoms-up' approach in the SLA also allowed us to use a variety of material compositions within the same structure for engineering the physical properties of the 3D matrix. It is now well-established that intrinsic mechanical properties of substrates have significant influences on the behavior of both somatic and stem cells in terms of development, differentiation, disease, and regeneration.[30,36] The promising results from these 2D experiments have given rise to new studies attempting to spatially control the physical properties in 3D. In a recent study, this was accomplished by sequential cross-linking of hyaluronic acid (HA) hydrogels using addition reactions and mask-based photoinitiated crosslinking. The result was a difference in mechanical properties stemming from variations in the cross-linking densities.[37] When a similar setup was used for stem cell encapsulation, cells with different morphologies on different regions of the hydrogel were obtained.[38] The fabrication process in our study may offer such control not only by varying the crosslinking density in different regions of the same material, but also by enabling the use of various types and concentrations of materials.

All PEGDA hydrogels tested in this study, except for M_w 700 Da, showed long-term viability for cells encapsulated over 14 days. The reason for poor viability in PEGDA with M_w 700 Da was most likely due to low degrees of swelling caused by small pore sizes. This restricted the diffusion of oxygen and nutrients into the inner core of the hydrogels. When PEGDA was functionalized with 5 mM RGDS at higher M_w, cells were not only viable, but they also spread and proliferated. Proliferation was observed through 7 days, followed by a decrease in the cell numbers after 14 days. A similar result was obtained when smooth muscle cells were encapsulated in RGDS-functionalized PEGDA hydrogels with M_w 3400 Da using bulk UV exposure.[39] Although there was a severe decrease in the initial cell viability after 24 hours, the same increasing trend in cell numbers were observed after 7 days. The initial decrease in their viability could have been due to cell damage caused by bulk polymerization conditions, such as the photoinitiator concentration, UV exposure time, and presence of organic solvents. The elastic modulus

of the hydrogels produced from 20% PEGDA with M_w 3400 Da in the study by Peyton *et al.*[39] was approximately 400 kPa, while the modulus in our study was approximately 17 kPa. This discrepancy could be due to variations in the polymerization process or even the method of measurement. The advantage of the SLA process is its precise control over the average energy dose, which can limit the adverse effects to cells.

In general, PEG hydrogels have many attractive properties, including excellent biocompatibility and hydrophilicity. Even though PEG is an inert molecule, cell-surface recognition sites can be chemically tailored to it in a controllable manner.[39] During SLA fabrication of multi-layer 3D hydrogels, the first and last layers of the 10-layer structure were made without RGDS, while the middle layers were made with RGDS. While this was done to prevent cell growth at the exterior of the hydrogels, it also demonstrates the ability to spatially organize bioactive molecules in multi-layer 3D structures. The addition of these adhesive molecules or other types of molecules regulating cell function into distinct layers can easily be achieved by using the 'bottoms-up' fabrication method in the SLA.

It should be noted that the PEG hydrogels used in this study were not biodegradable, which could have prevented further cell proliferation and extensive network formation. This may have been the reason for the decrease in cell viability after 14 days. Future studies can incorporate biodegradable matrix molecules or sequences within the hydrogels during the SLA process. Another reason for the decrease in cell viability after 14 days may have been the constraints caused by low nutrient and waste transport in the hydrogels. Although PEG hydrogels used in our studies had high enough porosity for the diffusion of small molecules up to 22 kDa,[11] including oxygen and glucose, MTT staining after 14 days suggested problems caused by diffusion because there were more cells located at the periphery than at the middle of the hydrogels. This effect was only seen in long-term cultures. A possible explanation may be the diffusion restrictions caused by larger molecules like ECM components secreted by the cells building up around the cells that were secreting them, thereby causing a decrease in the diffusion of smaller M_w compounds. These issues can be overcome by providing degradable units in the PEG hydrogels. There are different methods reported in literature to render PEG degradable by including short peptides in its backbone for enzymatic cleavage by the encapsulated cells[40] or by making a copolymer with a hydrolytically degradable polymer like PLA.[8] A recent study supported this discussion by showing that SMCs and mesenchymal stem cells encapsulated in enzymatically degradable PEG possessed high cell spreading, network formation, and expression of matrix metalloproteinases for up to 21 days in culture.[40] Therefore, providing degradability in the hydrogels and combining that with our current technology could be the next step forward.

Conclusion

A custom-modified SLA was used to fabricate complex 3D structures from photopolymerizable PEG hydrogels to accommodate for two fabrication methods: (1) the 'top-down' approach, which employs a process similar to the conventional SLA, and (2) the 'bottoms-up' approach, which allows for multiple types of cells and polymers to be arranged in their own layers within a structure. NIH/3T3 cells were successfully encapsulated within these structures, and by increasing the M_w of PEG and covalent linkage of bioactive RGDS groups, the cell viability, proliferation, and spreading were greatly improved over 14 days. The variation in PEG M_w also established the ability to tune the elasticity of the hydrogel to specific tissue types without sacrificing viability. The SLA is an enabling tool with excellent spatial control that can potentially be used to recapitulate the complex 3D hierarchy of the tissue microenvironment. This may have significant impact on driving the development of *in vitro* 3D models toward broader applications, including those in tissue engineering, cell mechanics, and bio-hybrid artificial devices and machines.

Acknowledgements

This project was made possible by a cooperative agreement that was awarded and administered by the US Army Medical Research & Materiel Command (USAMRMC) and the Telemedicine & Advanced Technology Research Center (TATRC), under Contract #: W81XWH0810701.

References

1 E. J. Suuronen, H. Sheardown, K. D. Newman, C. R. McLaughlin and M. Griffith, Building *in vitro* models of organs, *Int. Rev. Cytol.*, 2005, **244**, 137–173.
2 J. L. Drury and D. J. Mooney, Hydrogels for tissue engineering: scaffold design variables and applications, *Biomaterials*, 2003, **24**(24), 4337–4351.
3 B. V. Slaughter, S. S. Khurshid, O. Z. Fisher, A. Khademhosseini and N. A. Peppas, Hydrogels in regenerative medicine, *Adv. Mater.*, 2009, **21**, 3307–3329.
4 C. C. Lin and K. S. Anseth, PEG hydrogels for the controlled release of biomolecules in regenerative medicine, *Pharm. Res.*, 2009, **26**(3), 631–643.
5 D. L. Hern and J. A. Hubbell, Incorporation of adhesion peptides into nonadhesive hydrogels useful for tissue resurfacing, *J. Biomed. Mater. Res.*, 1998, **39**, 266–276.
6 B. K. Mann, A. S. Gobin, A. T. Tsai, R. H. Schmedlen and J. L. West, Smooth muscle cell growth in photopolymerized hydrogels with cell adhesive and proteolytically degradable domains: synthetic ECM analogs for tissue engineering, *Biomaterials*, 2001, **22**, 3045–3051.
7 E. A. Phelps, N. Landázur, P. M. Thule, R. Taylor and A. J. García, Bioartificial matrices for therapeutic vascularization, *Proc. Natl. Acad. Sci. U. S. A.*, 2010, **107**(8), 3323–3328.
8 A. T. Metters, K. S. Anseth and C. N. Bowman, Fundamental studies of a novel, biodegradable PEG-*b*-PLA hydrogel, *Polymer*, 2000, **41**, 3993–4004.
9 J. L. West and J. A. Hubbell, Polymeric biomaterials with degradation sites for proteases involved in cell migration, *Macromolecules*, 1999, **32**, 241–244.
10 G. P. Raeber, M. P. Lutolf and J. A. Hubbell, Molecularly engineered PEG hydrogels: a novel model system for proteolytically mediated cell migration, *Biophys. J.*, 2005, **89**, 1374–1388.
11 G. M. Cruise, D. S. Scharp and J. A. Hubbell, Characterization of permeability and network structure of interfacially photopolymerized poly(ethylene glycol) diacrylate hydrogels, *Biomaterials*, 1998, **19**(14), 1287–1294.
12 J. L. Ifkovits and J. A. Burdick, Review: photopolymerizable and degradable biomaterials for tissue engineering applications, *Tissue Eng.*, 2007, **13**(10), 2369–2385.
13 Y. Du, E. Lo, S. Ali and A. Khademhosseini, Directed assembly of cell-laden microgels for fabrication of 3D tissue constructs, *Proc. Natl. Acad. Sci. U. S. A.*, 2008, **105**(28), 9522–9527.
14 M. S. Hahn, J. S. Miller and J. L. West, Three-dimensional biochemical and biomechanical patterning of hydrogels for guiding cell behavior, *Adv. Mater.*, 2006, **18**, 2679–2684.

15 V. L. Tsang, A. A. Chen, L. M. Cho, K. D. Jadin, R. L. Sah and S. DeLong, et al., Fabrication of 3D hepatic tissues by additive photopatterning of cellular hydrogels, *FASEB J.*, 2007, **21**(3), 790–801.
16 V. L. Tsang and S. N. Bhatia, Fabrication of three-dimensional tissues, *Adv. Biochem. Eng./Biotechnol.*, 2006, **103**, 189–205.
17 S. M. Peltola, F. P. Melchels, D. W. Grijpma and M. Kellomäki, A review of rapid prototyping techniques for tissue engineering purposes, *Ann. Med.*, 2008, **40**(4), 268–280.
18 J. J. Pancrazio, F. Wang and C. A. Kelley, Enabling tools for tissue engineering, *Biosens. Bioelectron.*, 2007, **22**(12), 2803–2811.
19 M. Rücker, M. W. Laschke, D. Junker, C. Carvalho, F. Tavassol and R. Mülhaupt, et al., Vascularization and biocompatibility of scaffolds consisting of different calcium phosphate compounds, *J. Biomed. Mater. Res., Part A*, 2008, **86a**(4), 1002–1011.
20 R. Yao, R. J. Zhang, Y. N. Yan and X. H. Wang, *In vitro* angiogenesis of 3D tissue engineered adipose tissue, *J. Bioact. Compat. Polym.*, 2009, **24**(1), 5–24.
21 P. Yang, C. Wang, Z. Shi, X. Huang, X. Dang and S. Xu, et al., Prefabrication of vascularized porous three-dimensional scaffold induced from rhVEGF(165): a preliminary study in rats, *Cells Tissues Organs*, 2009, **189**(5), 327–337.
22 E. A. Silva and D. J. Mooney, Effects of VEGF temporal and spatial presentation on angiogenesis, *Biomaterials*, 2010, **31**(6), 1235–1241.
23 K. Kyriakidou, G. Lucarini, A. Zizzi, E. Salvolini, M. M. Belmonte and F. Mollica, et al., Dynamic co-seeding of osteoblast and endothelial cells on 3D polycaprolactone scaffolds for enhanced bone tissue engineering, *J. Bioact. Compat. Polym.*, 2008, **23**(3), 227–243.
24 K. F. Leong, C. K. Chua, N. Sudarmadji and W. Y. Yeong, Engineering functionally graded tissue engineering scaffolds, *J. Mech. Behav. Biomed. Mater.*, 2008, **1**(2), 140–152.
25 M. N. Cooke, J. P. Fisher, D. Dean, C. Rimnac and A. G. Mikos, Use of stereolithography to manufacture critical-sized 3D biodegradable scaffolds for bone ingrowth, *J. Biomed. Mater. Res.*, 2003, **64b**(2), 65–69.
26 B. Dhariwala, E. Hunt and T. Boland, Rapid prototyping of tissue-engineering constructs, using photopolymerizable hydrogels and stereolithography, *Tissue Eng.*, 2004, **10**(9/10), 1316–1322.
27 K. Arcaute, B. K. Mann and R. B. Wicker, Stereolithography of three-dimensional bioactive poly(ethylene glycol) constructs with encapsulated cells, *Ann. Biomed. Eng.*, 2006, **34**(9), 1429–1441.
28 G. Mapili, Y. Lu, S. Chen and K. Roy, Laser-layered microfabrication of spatially patterned functionalized tissue-engineering scaffolds, *J. Biomed. Mater. Res., Part B*, 2005, **75**(2), 414–424.
29 C. Chu, B. W. Schaefer, R. J. DeVolder and H. J. Kong, Quantitative analysis of the cross-linked structure of microgels using fluorescent probes, *Polymer*, 2009, **50**, 5288–5292.
30 D. E. Discher, P. Janmey and Y. L. Wang, Tissue cells feel and respond to the stiffness of their substrate, *Science*, 2005, **310**(5751), 1139–1143.
31 J. McGrath, Cell spreading: the power to simplify, *Curr. Biol.*, 2007, **17**(10), R357–R358.
32 H. N. Yang, J. S. Park, K. Na, D. G. Woo, Y. D. Kwon and K. H. Park, The use of green fluorescence gene (GFP)-modified rabbit mesenchymal stem cells (rMSCs) co-cultured with chondrocytes in hydrogel constructs to reveal the chondrogenesis of MSCs, *Biomaterials*, 2009, **30**(31), 6374–6385.
33 X. T. Mo, S. C. Guo, H. Q. Xie, L. Deng, W. Zhi and Z. Xiang, et al., Variations in the ratios of co-cultured mesenchymal stem cells and chondrocytes regulate the expression of cartilaginous and osseous phenotype in alginate constructs, *Bone*, 2009, **45**(1), 42–51.
34 S. A. Lee, S. E. Chung, W. Park, S. H. Lee and S. Kwon, Three-dimensional fabrication of heterogeneous microstructures using soft membrane deformation and optofluidic maskless lithography, *Lab Chip*, 2009, **9**(12), 1670–1675.
35 J. Fukuda, A. Khademhosseini, Y. Yeo, X. Yang, J. Yeh and G. Eng, et al., Micromolding of photocrosslinkable chitosan hydrogel for spheroid microarray and co-cultures, *Biomaterials*, 2006, **27**(30), 5259–5267.
36 A. J. Engler, S. Sen, H. L. Sweeney and D. E. Discher, Matrix elasticity directs stem cell lineage specification, *Cell*, 2006, **126**(4), 677–689.
37 S. Khetan, J. S. Katz and J. A. Burdick, Sequential crosslinking to controlcellular spreading in 3-dimensional hydrogels, *Soft Matter*, 2009, **5**, 1601–1606.
38 R. A. Marklein and J. A. Burdick, Spatially controlled hydrogel mechanics to modulate stem cell interactions, *Soft Matter*, 2010, **6**, 136–143.
39 S. R. Peyton, C. B. Raub, V. P. Keschrumrus and A. J. Putnam, The use of poly(ethylene glycol) hydrogels to investigate the impact of ECM chemistry and mechanics on smooth muscle cells, *Biomaterials*, 2006, **27**(28), 4881–4893.
40 C. Adelöw, T. Segura, J. A. Hubbell and P. Frey, The effect of enzymatically degradable poly(ethylene glycol) hydrogels on smooth muscle cell phenotype, *Biomaterials*, 2008, **29**(3), 314–326.

